



**Simple, Highly-Efficient Route to Electroless Gold Plating on
Complex 3D Printed Polyacrylate Plastics**

Journal:	<i>ChemComm</i>
Manuscript ID	CC-COM-07-2018-005368.R1
Article Type:	Communication

SCHOLARONE™
Manuscripts



Journal Name

COMMUNICATION

Simple, Highly-Efficient Route to Electroless Gold Plating on Complex 3D Printed Polyacrylate Plastics

Received 00th January 20xx,
Accepted 00th January 20xx

DOI: 10.1039/x0xx00000x

www.rsc.org/

Sung Ho Kim,* Julie Jackson, James S. Oakdale, Jean-Baptiste Forien, Jeremy M. Lenhardt, Jae-Hyuck Yoo, Swanee J. Shin, Xavier Lepró, Bryan D. Moran, Chantel M. Aracne-Ruddle, Theodore F. Baumann, Ogden S. Jones, and Juergen Biener

Compared to tedious, multi-step treatments for electroless gold plating of traditional thermoplastics, this paper describes a simpler three-step procedure for 3D printed crosslinked polyacrylate substrates. This allows for the synthesis of ultralight gold foam microlattice with great potential to architecture-sensitive applications in future energy, catalysis, and sensing.

Three-dimensional (3D) polymer-based printing technologies coupled with electroless metal plating (ELP) have provided a new fascinating pathway to fabricate ultralight metallic microlattice materials with tailored architectures and unique properties.^{1,2} Despite the still relatively large feature size of both ligaments and pores in printed polymer parts, the rapidly developing 3D printing technologies have great potential to replace current synthetic strategies for low-density metal foams because of unprecedented digital control to fabricate complex 3D objects without the need for expensive tooling or machining. However, it requires some sort of metal coating of polymer substrates to obtain the desired metal parts. So far, most work in this field focused on thermoplastic polymers that were used in fused deposition modeling (FDM) and selective laser sintering (SLS), including acrylonitrile-butadiene-styrene (ABS), polylactic acid (PLA), poly(ethylene terephthalate) (PET), and polyethylene terephthalate glycol-modified (PETG).^{3,4} Studies on high-resolution 3D techniques such as stereolithography (SL) and two photon lithography (TPL) were still limited despite their better surface finish and higher resolution.^{5,6} This might be attributed to the fact that these methods depended on photopolymerization of UV-curable monomers that formed highly crosslinked insoluble polymer networks. Electroless plating is a catalytic, redox reaction of metal ion in an aqueous solution with a reducing chemical agent. It is theoretically possible for any metal to be deposited or plated on polymer substrates given that the surface of

polymers is properly prepared to provide an appropriate catalyst (typically noble metals, e.g. palladium, platinum, gold) for electroless plating.^{7,8} However, electroless nickel (Ni) and copper (Cu)-plating dominated the recent literature.⁸ We had developed various low-density metal foams by using micrometer-sized polymer beads as a sacrificial template.^{9,10} Developing efficient electroless metal plating capabilities of the polymer templates was vital to achieving our goals. Here, we develop a simple, versatile route to electroless gold (Au) plating on crosslinked polyacrylate-based substrates which are printed by either projection microstereolithography (PμSL) or TPL, which were suitable for printing large-area, high-resolution structures. Despite the high price of gold, approaches to prepare uniform gold patterns have been indispensable for microelectronic industries.⁸ Gold foams have been excellent catalysts,¹¹ and critical components in high energy-density physics (HED) and inertial confinement fusion (ICF) experiments for future energy applications.^{9,10}

The conventional and commercially available procedure for electroless plating on the molded plastic part required tedious, multi-step treatments to overcome the inherent lack of adhesion of a catalytic metal seed onto the polymer substrate.^{7,8} There have been many efforts to improve or even eliminate these harsh treatments.^{12,13} For example, Wang et al. developed an initiator-integrated 3D printing approach to grow polyelectrolyte brushes on initiator-integrated 3D samples via surface-initiated polymerization.¹² They indicated that both a strong electrostatic interaction and surface chemistry improved the adhesion. Another difficulty was that the baths and solutions used for electroless gold plating typically contained many components including metal complex ions, reducing agents, pH adjustment and buffering components, and other additives, requiring elevated temperature treatments.^{7,14}

* Lawrence Livermore National Laboratory, 7000 East Avenue, Livermore, California 94550, USA. E-mail: kim61@llnl.gov

† Electronic Supplementary Information (ESI) available: details on material preparation and characterization; additional SEM images; nanoindentation; electrical conductivity. See DOI: 10.1039/x0xx00000x

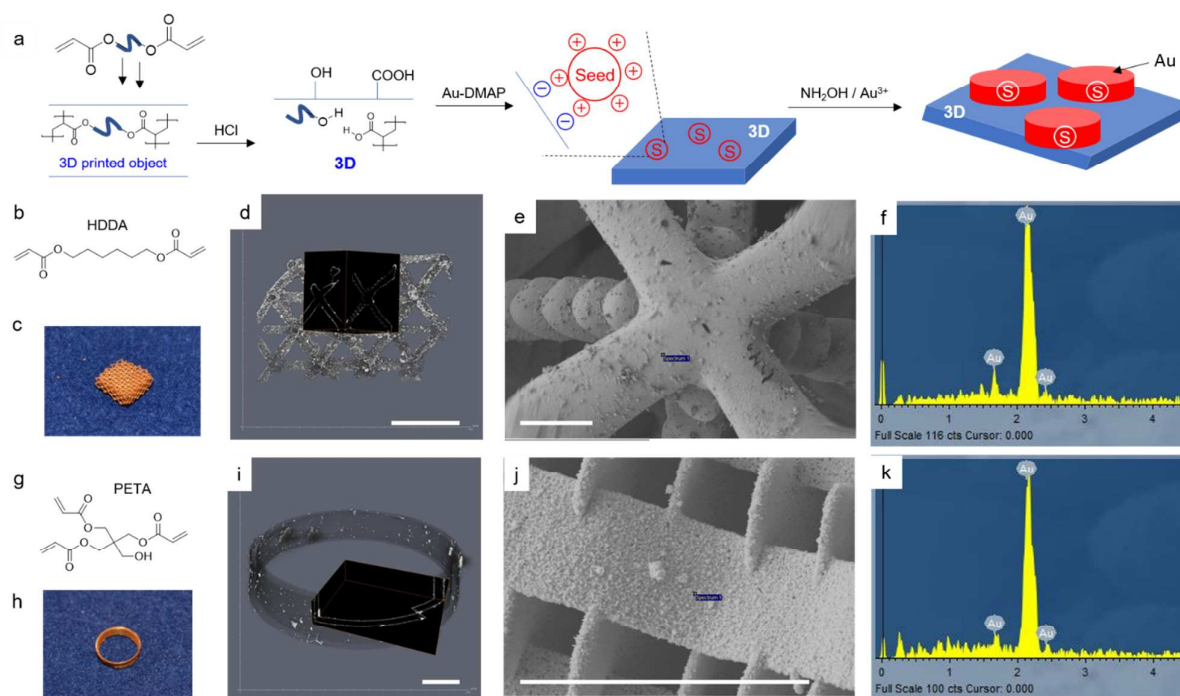


Fig.1 Au Electroless plating of 3D printed polyacrylates. (a) Schematic representation of our three-step procedure. (b–k) Chemical structures of multi-acrylate resins (HDDA or PETA), and typical photos, X-ray CT, and SEM/EDS images for Au-coated 3D architectures (HDDA-Au or PETA-Au). Scale bars are 1 mm (d,i), 100 μm (e), and 10 μm (j).

Our three-step procedure for forming gold coatings on 3D printed polyacrylate substrates is shown in Fig. 1a: (i) surface modification of a substrate, (ii) seeding with gold nanoparticles, and (iii) electroless Au plating of the seeded substrate. This approach took advantage of the strong electrostatic interaction between the negatively charged 3D polymer substrate and the positively charged Au-DMAP nanoparticle seed. 3D printed polyacrylates were surface-functionalized via HCl treatment to introduce $-\text{COOH}$ functional groups on the polymer surface.^{15,16} Colloidally stable, water-soluble dimethylaminopyridine-functionalized gold nanoparticles (Au-DMAP) were prepared by Gittins and Caruso's method.¹⁷ The Au-DMAP nanoparticles (~ 5 nm diameter) were positively charged within the pH range of 7 to 12.¹⁷ Subsequent electroless Au plating was carried out using an aqueous mixture of HAuCl_4 and $\text{NH}_2\text{OH}\cdot\text{HCl}$ at room temperature, as similarly to Brown and Natan's hydroxylamine method.¹⁸ An initial substrate is 1,6-hexanediol diacrylate (HDDA)-based 3D object printed via P μ SL (Fig. 1b).¹⁹ Fig. 1c–1f are optical, reconstructed X-ray computed tomography (CT), and SEM/EDS images of a gold-coated porous HDDA structure (HDDA-Au, $5 \times 5 \times 2$ mm³, 150 μm line width). Typically, the surface of the gold-coated sample is shiny with a metallic, yellowish color. No noticeable volume change nor distortion are observed during air drying at ambient condition. X-ray CT was used to monitor 3D distribution of the gold coatings in the sample. Specifically, a bright color represents the gold. Fig. 1d shows the Au coatings are uniformly formed throughout the HDDA substrate. The SEM micrograph and corresponding EDS energy spectrum of Fig. 1e and 1f confirm further details on smooth, conformal Au coatings. We are also successful in

forming an Au coating on a different kind of polyacrylate-based 3D sample prepared by TPL. The TPL was capable of printing much higher resolution of a polymer foam cylinder (200 μm thickness, sub- μm feature size) using commercial resin, which was primarily composed of pentaerythritol triacrylate (PETA) (Fig. 1g). The results of Fig. 1h–1k demonstrate the versatility of our approach (Full details on experimental procedure in ESI).

Our approach was based on acid-catalyzed ester hydrolysis, as reported in acetates, poly(methyl methacrylate), and poly(lactic acid).^{15,16} As shown in the SEM micrographs of Fig. 2a–2b, it is obvious that the HCl treatment increased the surface roughness. The origin of the surface roughening is revealed by monitoring the ATR-IR spectra for HDDA-based samples before and after acid treatment (Fig. 2c). The evolution of a new O–H peak in the modified sample confirms that acid-catalyzed ester hydrolysis occurs and increases the surface concentration of carboxylic acid groups despite highly-crosslinked, water-insoluble nature of the HDDA part. We observed that this modification was inherently limited to the surface irrespective of a reaction time (up to ~ 5 days) when the reaction was performed at room temperature. It is worth mentioning that we also tried other surface modification routes such as base hydrolysis (aqueous NaOH at 1 M and 6 M) and oxygen plasma treatment. None of those attempts was as effective as HCl treatment.

Acid dissociation constant, pK_a , of acrylic acid is between 4 and 5. At a neutral pH 7, most of carboxylic acid is in the form of its conjugate base (COO^-) (see the Henderson-Hasselbalch equation, ESI). The presence of carboxylate anions on the surface of the modified 3D printed structure facilitated the

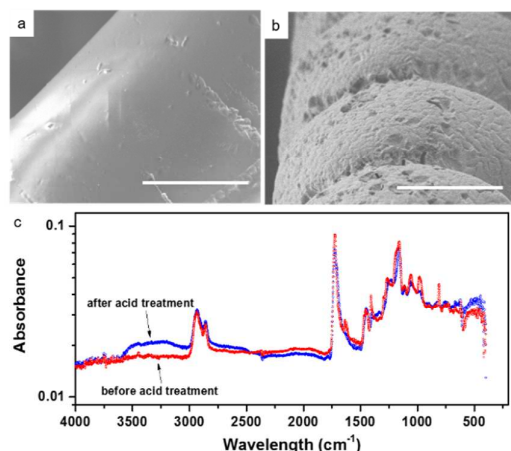


Fig. 2 Surface modification of 3D printed polyacrylates with HCl treatment. (a-c) SEM images and ATR-IR spectra of the HDDA sample before (a) and after acid treatment (b). Scale bar is 50 μm (a,b).

strong adhesion of the positively-charged Au nanoparticles (catalysts). For electroless gold plating on the seeded substrate, we used the hydroxylamine method to reduce Au³⁺ by NH₂OH.¹⁸ This protocol had several advantages over conventional gold plating formulas based on gold cyanide or sulfite baths.¹⁴ For example, it uses aqueous solutions of HAuCl₄ and NH₂OH·HCl without other additives, and the plating reaction proceeded rapidly at room temperature in a few minutes. Fig. 3 shows the effect of a surface treatment on the surface morphology of 3D-printed samples after electroless Au plating. In SEM images, the gold has a bright color while uncoated polymer has a dark color due to surface charging (Fig. S1, ESI). The untreated HDDA at both low and high magnifications reveals the presence of large isolated gold particles (Fig. 3a and 3b). The hydroxylamine method was initially developed to grow existing Au nanoparticles (seeds) into larger particles based on the dramatically accelerated reduction of Au³⁺ on the Au surface. The large Au particles observed after electroless plating reflect the initial distribution of the seeds (Au-DMAP nanoparticle) adsorbed on the substrate.¹⁸ Without proper pre-treatment, weakly-adsorbed Au-DMAP catalysts and large Au particles seem to be easily detached during washing steps, thus producing poor-quality, non-uniform metallic coatings. By contrast, smooth, conformal, complete gold coatings are obtained on the acid-treated HDDA sample (Fig. 3c and 3d). This enhanced adhesion could be explained by a combination of the improved mechanical interlocking due to surface roughness and the favourable chemical interaction due to ester hydrolysis. Additional SEM images at high magnifications show that the Au thin film is composed of densely-packed smaller grains in size of ~100 nm, and it has a slight surface roughness (Fig. S2, ESI). Interestingly, we observed that a conventional tin/palladium (Sn²⁺/Pd²⁺) activation could be successfully combined with the hydroxylamine method (Fig. S3, ESI). Despite potential advantages of tin sensitization such as accessibility and photo-selective metal deposition,²⁰ the gold

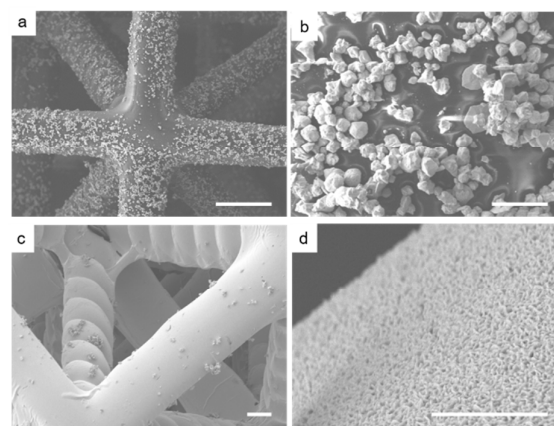


Fig. 3 Au electroless plating on polymers. (a, b) untreated HDDA and (c, d) acid-treated HDDA were used as a substrate. Scale bars are 50 μm (a,c) and 5 μm (b,d).

nanoparticle seeding was still preferred in this study because of a strict composition requirement to our specific application.

Thermogravimetric analysis (TGA) of HDDA and HDDA-Au samples in Fig. 4a reveals that the HDDA polymer completely decomposed below 600 °C. The initial weight loss observed for HDDA in the 150-200 °C range was attributed to unreacted, volatile resin components. The TGA weight at 800 °C was further used to estimate the initial Au thickness of the HDDA-Au. Assuming a simple cylindrical strut geometry (150 μm diameter), the Au coating thickness of the HDDA-Au prepared by our standard condition (at 5 min plating time and 10 mg Au salt) was determined to be about ~0.4 μm . To gain additional control over the formation of Au coatings, we also investigated the effect of time and concentration on the thickness of Au coatings (Fig. S3 and Table S1, ESI). The Au plating reaction of this study occurs quite fast, and an early time increase from 1 min to 5 min caused 3 \times thickness increase. However, it was almost completed in ~5 min and further time increase up to ~60 min did not cause a drastic change. Adding more Au salts to a plating solution effectively increased the Au thickness up to ~0.80 μm . Based on the TGA data, the sacrificial polymer

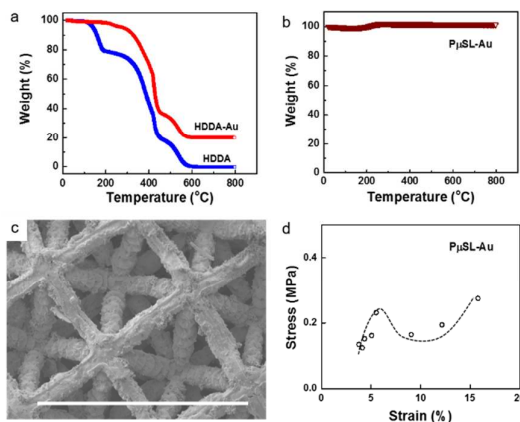


Fig. 4 Formation of 3D Au foam. (a, b) TGA curves of HDDA, HDDA-Au, and P1SL-Au foams (c) SEM image and (d) indentation stress-strain curve of the P1SL-Au. Scale bar is 500 μm (c).

template, HDDA, was removed by baking at 400 °C for 8 h in air. The resulting gold foam is called P μ SL-Au, named after the printing technique. No additional weight loss is observed in the TGA curve (Fig. 4b), indicating the 400 °C baking step completely removed the polymer. After the thermal baking process, the P μ SL-Au becomes one-third size of the HDDA-Au (Fig. S4, ESI). Despite the pronounced shrinkage, it is isotropic, and the macroscopic monolithic shape is retained. No large crack formation is observed, and the typical gold foam sample has a very low density of 0.6 \pm 0.1 g/cm³ (3-4% relative to full density Au) (Table S2, ESI). Fig. 4c is SEM images of gold foams after the thermal baking process. We observe the decrease in the strut size from \sim 150 μ m in the HDDA template to \sim 50 μ m in the P μ SL-Au. Additional SEM images at high magnifications reveals that sintering at an elevated temperature resulted in the grain size increase, ranging from hundreds of nm to 1 μ m (Fig. S5, ESI). While the P μ SL template with relatively large feature size resulted in the formation of uniform gold foams, much smaller feature size of the TPL substrate showed the preferential gold deposition on the inner/outer surface, although the inside was also coated with the gold (Fig. S6 and S7, ESI). Inhomogeneity of the gold film at different sample parts does not only pose a problem, but it also presents a new opportunity, allowing the preparation of deposits with defined nanostructure. We also attempted chemical etching of HDDA-Au using a strong base at elevated temperature (aqueous 6M NaOH or 1% triazabicyclodecene (TBD) in ethylene glycol), but they were not successful in selectively removing polymers because of the fragility of our plated gold under the condition.

Here, we tried to measure several other properties for the typical P μ SL-Au sample (\sim 0.6 g/cm³ density). Fig. 4d shows a stress-strain curve obtained from nanoindentation (see Nanoindentation, ESI). Interestingly, the curve clearly shows a presence of yield point, and we observed a sudden increase in the displacement without a significant load increase in the load-displacement curve (Fig. S8, ESI). This behavior is typical of a material that cold-draws with necking down the cross-section in a limited area of the specimen. This might be due to a unique highly porous, tubular morphology of our 3D gold foams. Young's modulus was obtained from the slope to be 5.3 \pm 1.6 MPa. Detailed comparison on the mechanical properties is above the scope of this study and will be treated in future publications. The Au foam has a high BET surface area of 2.0 \times 10⁷ m² m⁻³ (or 33 \pm 6 m²/g at \sim 0.6 g/cm³). This exceeds commercially available metal sponges by a factor of 1,000-10,000.²¹ The gold foam is so conductive that it was not possible to directly measure a resistance using a multi-meter. Here, we developed a simple experimental set-up to measure electric conductivity (see Electric conductivity, Fig. S9, ESI). The conductivity was determined to be \sim 9.0 \times 10³ S/m. It has a very good electrical conductivity although the value was still \sim 2 orders of magnitude smaller than a theoretical maximum of the gold.

In summary, we developed a simplified, highly efficient process for gold electroless plating of crosslinked polyacrylate-based 3D printed objects. The direct polymer modification route described in this paper did not require any changes to

the formulation of widespread UV-curable acrylate resins and can be easily applied to a variety of different polyacrylate-based architectures printed by other 3D printing techniques. Our approach required only a few components and worked at room temperature. This provides significant advantage over conventional or commercial electroless plating baths that contained many components. Uniform Au coatings on complex polymer architectures as well as ultralight, highly-conductive, high surface area gold foams will open many new exciting opportunities to benefit both academia and industries in areas of materials science, catalysis, microelectronics, and energy applications.

This work was performed under the auspices of the U.S. Department of Energy by Lawrence Livermore National Laboratory under Contract DE-AC52-07NA27344.

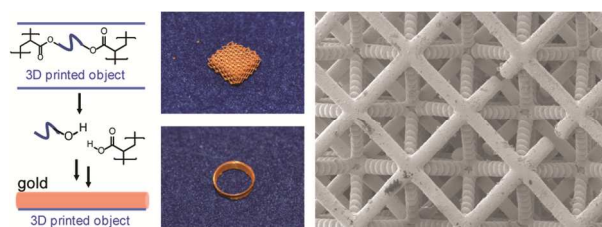
Conflicts of interest

There are no conflicts to declare.

Notes and references

- 1 T. A. Schaedler, A. J. Jacobsen, A. Torrents, A. E. Sorensen, J. Lian, J. R. Greer, L. Valdevit, W. B. Carter, *Science*, 2011, **334**, 962.
- 2 X. Zheng, W. Smith, J. Jackson, B. Moran, H. Cui, D. Chen, J. Ye, N. Fang, N. Rodriguez, T. Weisgraber, C. M. Spadaccini, *Nat. Mater.*, 2016, **15**, 1100.
- 3 A. Equbal, A. Sood, *Coatings*, 2014, **4**, 574.
- 4 R. Bernasconi, G. Natale, M. Levi, L. Magagnin, *J. Electrochem. Soc.*, 2016, **163**, D526.
- 5 R. Bernasconi, C. Credi, M. Tironi, M. Levi, L. Magagnin, *J. Electrochem. Soc.*, 2017, **164**, B3059.
- 6 B. Luan, M. Yeung, W. Wells, X. Liu, *Appl. Surf. Sci.*, 2000, **156**, 26.
- 7 G. O. Mallory, J. B. Hajdu, *Electroless Plating: Fundamentals and Application*, American Electroplaters and Surface Finishers Society, Florida, 2009.
- 8 Y. Shacham-Diamand, T. Osaka, Y. Okinaka, A. Sugiyama, V. Dubin, *Microelectron. Eng.*, 2015, **132**, 35.
- 9 G. W. Nycy, J. R. Hayes, A. V. Hamza, J. H. Satcher, *Chem. Mat.*, 2007, **19**, 344.
- 10 S. H. Kim, N. Bazin, J. I. Shaw, J. H. Yoo, M. A. Worsley, J. H. Satcher, J. D. Sain, J. D. Kuntz, S. O. Kucheyev, T. F. Baumann, A. V. Hamza, *ACS Appl. Mater. Interfaces*, 2016, **8**, 34706.
- 11 J. Biener, M. M. Biener, R. J. Madix, C. M. Friend, *ACS Catal.*, 2015, **5**, 6263-6270.
- 12 X. Wang, Q. Guo, X. Cai, S. Zhou, B. Kobe, J. Yang, *ACS Appl. Mater. Interfaces*, 2014, **6**, 2583.
- 13 F. Basarir, *ACS Appl. Mater. Interfaces*, 2012, **4**, 1324.
- 14 Y. Okinaka, M. Hoshino, *Gold Bull.*, 1998, **31**, 3.
- 15 H. Tsuji, K. Nakahara, *J. Appl. Polym. Sci.*, 2002, **86**, 186.
- 16 T. I. Croll, A. J. O'Connor, G. W. Stevens, J. J. Cooper-White, *Biomacromolecules*, 2004, **5**, 463.
- 17 D. I. Gittins, F. Caruso, *Angew. Chem. Int. Edit.*, 2001, **40**, 3001.
- 18 K. R. Brown, M. J. Natan, *Langmuir*, 1998, **14**, 726.
- 19 X. Zheng, J. Deotte, M. P. Alonso, G. R. Farquar, T. H. Weisgraber, S. Gemberling, H. Lee, N. Fang, C. M. Spadaccini, *Rev. Sci. Instrum.*, 2012, **83**, 125001.
- 20 X. Wei, D. K. Roper, *J. Electrochem. Soc.*, 2014, **161**, D235.
- 21 B. Dietrich, *Chem. Eng. Sci.* 2012, **74**, 192.

Table of Contents Entry



We develop simple, highly-efficient route to electroless gold plating on complex 3d printed polyacrylate plastics.